

A SPECTROSCOPIC AND SEMIEMPIRICAL QUANTUM CHEMICAL STUDY OF COPPER(II) PHTHALOCYANINATE

Andrei Racu^{1,2*}, Mihai-Cosmin Pascariu^{1,3}, Zoltán Szabadai^{1,4*}, Mircea Mracec⁵

¹*Renewable Energies - Photovoltaic Laboratory, National Institute of Research & Development for Electrochemistry and Condensed Matter – INCEMC Timișoara, 144 Dr. Aurel Păunescu-Podeanu, RO-300569 Timișoara, Romania*

²*Institute of Applied Physics of the Academy of Sciences of Moldova, 5 Academiei, MD-2028 Chișinău, Moldova*

³*Faculty of Pharmacy, “Vasile Goldiș” Western University of Arad, 86 Liviu Rebreanu, RO-310414 Arad, Romania*

⁴*Faculty of Pharmacy, “Victor Babeș” University of Medicine and Pharmacy of Timișoara, 2 Eftimie Murgu Sq., RO-300041 Timișoara, Romania*

⁵*Department of Computational Chemistry, Institute of Chemistry Timișoara of Romanian Academy, 24 Mihai Viteazul Av., RO-300223 Timișoara, Romania
e-mail: andrei.racu@gmail.com, szabadai@umft.ro*

Abstract

Copper(II) phthalocyaninate (CuPc) was studied using both the PM3 and PM7 semiempirical molecular orbital methods, and the results were compared with its XRD, FTIR and Raman experimental properties.

Introduction

Organic semiconductors are intensively studied for applications in electronics, optics and spin-based information technology (spintronics) [1]. Among these materials, the blue pigment copper(II) phthalocyaninate (CuPc) is a common, low-cost and chemically modifiable p-type organic semiconductor [1,2].

CuPc (Fig. 1) exhibits a planar molecule consisting of a central metal atom bound to a ligand with extended π conjugated system [2,3]. It shows good thermal and chemical stability and can be easily deposited as a thin film [2] when its performance proves to be superior to that of single-molecule magnets over the same temperature range [1]. It thus holds promise for quantum information processing and medium-term storage of classical bits in all-organic devices on plastic substrates [1]. CuPc nanoribbons can also be fabricated using vapor phase deposition and these were studied for photoluminescence, with significant differences in the luminescent behavior being found between α -CuPc and β -CuPc nanostructures [3].

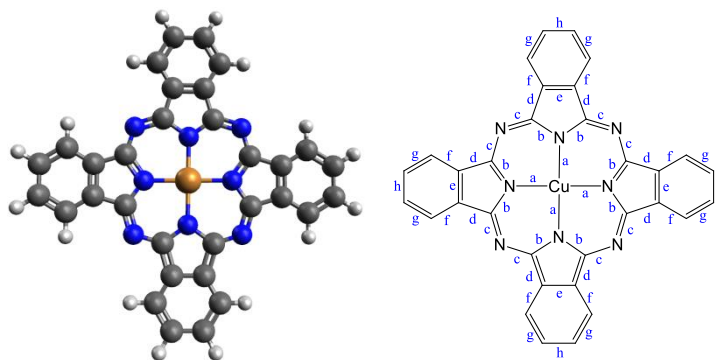


Figure 1. Molecular model (PM7) and notation of bonds for CuPc

In the past decades, the organic light-emitting diodes (OLEDs) based on CuPc as a buffer, hole injection or emitting layer, the organic solar cells (OSCs) based on CuPc as a donor material and the organic field-effect transistors (OFETs) based on CuPc as an active layer have been extensively studied due to this compound's interesting photoelectric properties: an optical gap (~ 1.7 eV) very suitable for visible absorption (i.e., usage in photovoltaic devices) and a transport gap (~ 2.3 eV) fit for electronic devices [2,3]. Near-infrared (NIR) photosensitive organic field-effect transistors based on CuPc/ErPc₂ heterojunction exhibit better properties when compared with the ErPc₂ single-layer ones, and thus good NIR photoresponsive layers can be obtained [2]. Also, the NIR light is intimately linked to industrial applications, such as NIR photodetectors and night vision [2].

In this paper, we use the PM3 and PM7 semiempirical molecular orbital methods to calculate some molecular properties of CuPc, like the bond lengths and the vibrational spectrum. We also compare the obtained results with the experimental spectroscopic data.

Experimental

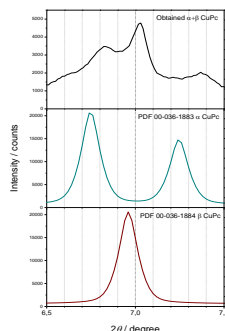
CuPc was obtained by using phthalic anhydride, copper(I) chloride, urea and ammonium molybdate, as described in the literature [4].

The UV/Vis spectrum (250–1000 nm) was acquired using an M-2000 (J.A. Woollam Co., USA) spectroscopic ellipsometer by diluting the sample with KBr, as pellets. The FTIR spectrum (400–4000 cm⁻¹) was also acquired using KBr pellets, on a Vertex 70 (Bruker, Germany) FT-IR spectrometer. The Raman spectrum was obtained at room temperature on a Multi Probe Imaging – MultiView 1000 scanned probe microscopy (Nanonics Imaging, Israel) system, which incorporates the Shamrock 500i Spectrograph (Andor, UK). A laser wavelength of 514.5 nm was used as the excitation source, with a 20 s exposure time and a 300 l mm⁻¹ grating. The XRD diffraction pattern was obtained on a X'Pert PRO MPD (Philips-FEI PANalytical Company, Netherlands) diffractometer.

The PM3 [5] optimization was performed by using the HyperChem software [6]. The SCF “Convergence limit” was set at 10⁻⁵ with an iteration limit of 100 and without using the “Accelerate convergence” procedure. For geometry optimization, the “Polak-Ribière (conjugate gradient)” algorithm was selected with an RMS gradient of 0.001 kcal/(Å mol).

For PM7 [7], the MOPAC2016 software [8] was used with the following keywords: CHARGE=0, PM7, DOUBLET, EF (or BFGS), OPT, BONDS, AUX, GRAPHF, PDBOUT, SCFCRT=1.D-10, PRECISE, GNORM=0.001, CYCLES=5000, LARGE. The BFGS (Broyden-Fletcher-Goldfarb-Shanno) algorithm gave very similar results with those obtained with the EF (Eigenvector Following) algorithm. Discarding the OPT keyword also gave very similar results in all cases. The Jmol [9] and Avogadro [10] programs were used for visualizing the molecular geometries.

Results and discussion



The powder XRD peaks (Fig. 2) indicate that the synthesized CuPc is a mixture of α and β phases, as seen when compared with the reference PDF data. The β -CuPc phase crystallizes in the monoclinic crystal system with space group P21/n and lattice parameters $a=14.64 \text{ \AA}$, $b=4.69 \text{ \AA}$, $c=17.31 \text{ \AA}$, $\alpha=90.00^\circ$, $\beta=105.49^\circ$, $\gamma=90.00^\circ$ [11]. α -CuPc crystallizes in the orthorhombic crystal system with lattice parameters $a=12.97 \text{ \AA}$, $b=12.15 \text{ \AA}$, $c=6.66 \text{ \AA}$ and $\alpha = \beta = \gamma = 90^\circ$ [12]. The selected $6.5\text{--}7.5^\circ 2\theta$ domain is suitable for the identification of α and β phases of CuPc.

Figure 2. Comparison between the obtained diffractogram and standard CuPc patterns. Differences between α and β phases of CuPc can also be revealed using optical absorption spectroscopy [3,13,14]. The obtained spectrum of CuPc (Fig. 3) consists of absorption peaks in the UV (B band) and red (Q band) spectral regions. One of the B band peaks is located at 330 nm, while the Q band has two peaks, located at 620 and 696 nm, in close agreement with the literature [3,15]. The peak at 620 nm in the Q band is assigned to the $\pi\text{--}\pi^*$ transition of the CuPc molecule, while assignment of the peak from 696 nm is still under discussion: a $\pi\text{--}\pi^*$ transition, an exciton peak, a surface state, a vibrational structure, and a Davydov splitting are possible candidates [15]. The difference between α and β phases of CuPc can be observed via the shape change of the Q band [3]. α phase shows a more intense absorption at lower wavelengths, while a pronounced absorption at a higher wavelength is specific for the β phase [12,14]. Taking in consideration the literature reported results, we can confirm that the obtained absorbance spectrum is an evidence that the obtained compound is a mixture of α - and β -CuPc [3].

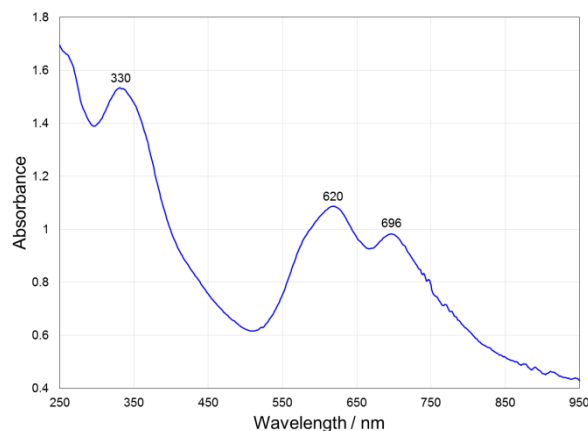


Figure 3. UV/Vis absorption spectrum of CuPc

The obtained Raman spectrum (Fig. 4) confirms the CuPc compound's formation, as seen in Table 1. The vibrational modes of Raman bands can be attributed to vibrations of the macrocycle, of the isoindole moieties, to C–H bendings and to the metal–nitrogen stretch.

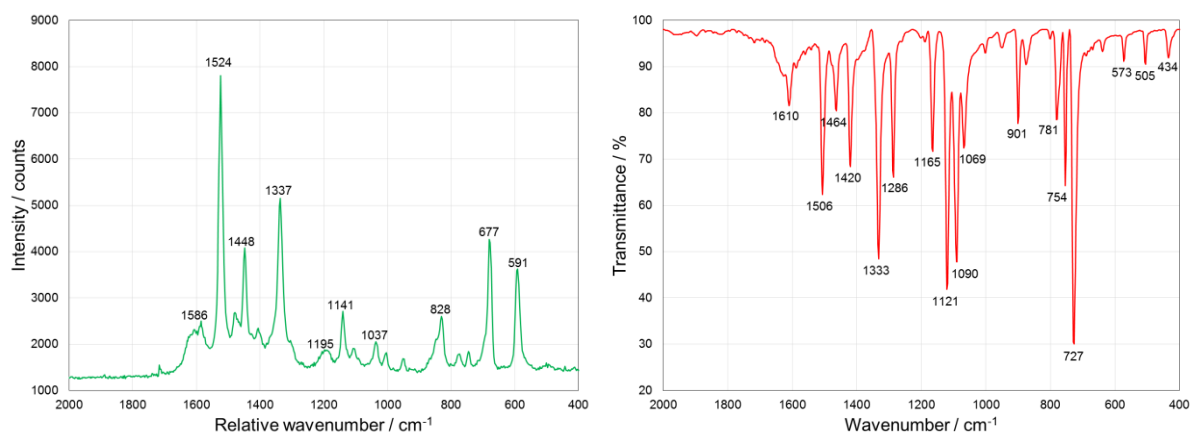


Figure 4. Raman (left) and FTIR (right) spectra of CuPc

Table 1. Raman lines identification and interpretation for CuPc

Our results	Literature results [16,17]			Interpretation
	β -CuPc powder	α -CuPc film	β -CuPc film	
$\alpha + \beta$ CuPc powder	β -CuPc powder	α -CuPc film	β -CuPc film	
Peak position (cm ⁻¹)	Peak position (cm ⁻¹)	Peak position (cm ⁻¹)	Peak position (cm ⁻¹)	
591	593	591	590	-
677	677	684	681	16 membered inner ring breathing
771	773	-	-	macrocycle deformation
828	830	839	833	C-N stretching (aza groups)
841	848	-	-	-
1004	1008	1010	1010	isoindole in-plane bending
1037	1036	1041	1040	C-H bending-isoindole group
1102	1108	1109	1104	C-H bending out of plane
1195	1193	-	-	isoindole in-plane bending
1337	1336	1338	1339	C $_{\alpha}$ -C $_{\beta}$ stretching pyrrole group
1403	1408	1414	1409	C-N stretching pyrrole group
1448	1448	-	-	C-N stretching
1524	1523	1527	1523	C $_{\alpha}$ -C $_{\beta}$ stretching pyrrole group
1586	1586	1589	1586	-

However, due to the small shift in the peak positions attributed to the α - and β -CuPc phases, this technique is not relevant for the identification of the CuPc phase.

The computed vibrational frequencies (PM7) and bond lengths (PM3 and PM7) for CuPc are shown in Table 2 and, respectively, Table 3.

Table 2. Simulated (PM7, with or without using the OPT keyword) and experimental vibrational frequencies for CuPc; the Raman and FTIR spectra of CuPc are shown in Fig. 4

EF		BFGS		Experimental FTIR/Raman*
w/ OPT	w/o OPT	w/ OPT	w/o OPT	
493.04 (1.2)	502.45 (1.0)	502.72 (1.1)	503.71 (1.1)	505 (w)/495 (w)
563.78 (2.0)	558.19 (1.8)	558.54 (1.9)	558.50 (1.8)	573 (w)/565 (sh)
				-/591 (s)
				681 (w)/677 (s)
726.59 (5.5)	727.91 (5.6)	728.04 (5.5)	727.56 (5.6)	727 (vs)/-
745.99 (1.0)	758.70 (1.3)	759.15 (1.3)	759.08 (1.3)	754 (m)/743 (w)
				781 (w)/771 (w)
819.83 (1.3)	822.18 (1.3)	820.21 (1.3)	823.04 (1.3)	800 (w)/828 (m)
				901 (w)/-
				1032 (w, sh)/1037 (w)
				1069 (m)/-
1101.13 (1.0)	1105.76 (0.8)	1105.30 (0.8)	1106.17 (0.8)	1090 (s)/1100 (w)
				1121 (s)/1124 (w, sh)
				-/1141 (m)
				1165 (m)/1157 (w, sh)
				1192 (w)/1195 (w)
1227.80 (1.4)	1227.36 (1.5)	1227.64 (1.4)	1227.76 (1.4)	
1276.59 (1.8)	1277.30 (1.9)	1276.76 (1.8)	1277.06 (1.9)	1286 (m)/-
1289.63 (2.4)	1291.75 (1.9)	1292.46 (2.0)	1291.97 (1.9)	
				1333 (s)/1337 (s)
1369.80 (2.5)	1373.59 (2.2)	1373.53 (2.1)	1373.93 (2.2)	
1403.36 (2.5)	1403.97 (3.8)	1404.40 (3.9)	1402.99 (3.9)	1420 (m)/1422 (w)
				-/1448 (s)
				1464 (w)/1477 (w)
				1506 (m)/-
				1518 (w)/1524 (vs)
1540.67 (2.4)	1541.27 (2.8)	1540.49 (3.5)	1541.00 (2.9)	
1559.21 (16.6)	1562.96 (15.6)	1561.26 (15.0)	1563.30 (15.5)	
				1587 (w)/1586 (w)
				1610 (w)/1601 (w)
1651.88 (8.5)	1647.03 (9.0)	1647.34 (8.6)	1646.89 (8.8)	
1712.49 (7.5)	1715.20 (6.7)	1714.84 (6.8)	1715.62 (6.8)	
1727.13 (7.8)	1729.34 (9.7)	1728.93 (9.7)	1729.61 (9.8)	

*w – weak, m – medium, s – strong, vs – very strong, sh – shoulder

Table 3. Computed and experimental bond lengths (in Å) for CuPc

Bond (see Fig. 1)	PM3 ($\Delta H_f = 132.641$ kcal/mol)	PM7 ($\Delta H_f = 240.303$ kcal/mol)	Experimental
a	1.899-1.900	1.982	1.950-1.953
b	1.401-1.487	1.367-1.423	1.379-1.389
c	1.331-1.353	1.326-1.341	1.344-1.371
d	1.443-1.464	1.469-1.485	1.441-1.490
e	1.417-1.420	1.425	1.407
f	1.387-1.397	1.377-1.381	1.377-1.399
g	1.394-1.399	1.403-1.405	1.372-1.401
h	1.398-1.403	1.393	1.399-1.412
C-H	1.094-1.096	1.089-1.091	-

Conclusion

CuPc was synthesized and spectroscopically analyzed. The XRD, Raman, FTIR and UV/Vis spectra confirmed the compound's identity. Both PM3 and PM7 gave good results regarding the molecular geometry. The vibrational spectra obtained with the PM7 method was only partially confirmed by the experimental FTIR and Raman spectra.

Acknowledgements

This work was supported by the Romanian National Authority for Scientific Research (CNCS-UEFISCDI) through project PN 16 14 03-10. We are gratefully acknowledging the generous support of J.J.P. Stewart for providing an academic license for the MOPAC2016.

References

- [1] M. Warner, S. Din, I.S. Tupitsyn, G.W. Morley, A.M. Stoneham, J.A. Gardener, Z. Wu, A.J. Fisher, S. Heutz, C.W.M. Kay, G. Aeppli, *Nature* 503 (2013) 504.
- [2] J. Zhang, Y. Li, Y. Tang, X. Luo, L. Sun, F. Zhao, J. Zhong, Y. Peng, *Synth. Met.* 218 (2016) 27.
- [3] W.Y. Tong, H.Y. Chen, A.B. Djurišić, A.M.C. Ng, H. Wang, S. Gwo, W.K. Chan, *Opt. Mater. (Amsterdam, Neth.)* 32 (2010) 924.
- [4] F. H. Moser, A. L. Thomas, *Phthalocyanine Compounds*, Reinhold, New York, 1963.
- [5] J.J.P. Stewart, PM3, in: *Encyclopedia of Computational Chemistry*, Wiley, 2002.
- [6] HyperChem™ Professional, Hypercube, Inc., 1115 NW 4th Street, Gainesville, Florida 32601, USA, version 8.0.10 for Windows.
- [7] J.J.P. Stewart, *J. Mol. Model.* 19 (2013) 1-32.
- [8] J.J.P. Stewart: MOPAC2016 (Version: 16.035W), Stewart Computational Chemistry, Colorado Springs, CO, USA, <http://OpenMOPAC.net/>.
- [9] Jmol: an open-source Java viewer for chemical structures in 3D, <http://www.jmol.org/>.
- [10] (a) Avogadro: an open-source molecular builder and visualization tool. Version 1.1.0, <http://avogadro.cc/>; (b) M.D. Hanwell, D.E. Curtis, D.C. Lonie, T. Vandermeersch, E. Zurek, G.R. Hutchison, *J. Cheminf.* 4 (2012) 17.
- [11] L. Ruiz-Ramirez, A. Martinez, J. Mendieta, J.L. Brioso, E. Estop, J.S. Chinchon, *Afinidad* 44 (1987) 45.
- [12] R. Prabakaran, R. Kesavamoorthy, G.L.N. Reddy, F.P. Xavier, *Phys. Status Solidi B* 229 (2002) 1175.

- [13] W.Y. Tong, A.B. Djurišić, M.H. Xie, A.C.M. Ng, K.Y. Cheung, W.K. Chan, Y.H. Leung, H.W. Lin, S. Gwo, *J. Phys. Chem. B* 110 (2006) 17406.
- [14] E.A. Lucia, F.D. Verderame, *J. Chem. Phys.* 48 (1968) 2674.
- [15] A.T. Davidson, *J. Chem. Phys.* 77 (1982) 168.
- [16] R. Prabakaran, R. Kesavamoorthy, G.L.N. Reddy, F.P. Xavier, *Phys. Status Solidi B* 229 (2002) 1175.
- [17] W. R. Scheidt, W. Dow, *J. Am. Chem. Soc.* 99 (1977) 1101.